



# Complex evolution of transient slip derived from precise tremor locations in western Shikoku, Japan

David R. Shelly and Gregory C. Beroza

*Department of Geophysics, Stanford University, 397 Panama Mall, Stanford, California 94305-2215, USA  
(beroza@pangea.stanford.edu)*

Satoshi Ide

*Department of Earth and Planetary Science, University of Tokyo, Hongo 7-3-1, Bunkyo-ku, Tokyo 113-0033, Japan*

[1] Transient slip events, which occur more slowly than traditional earthquakes, are increasingly being recognized as important components of strain release on faults and may substantially impact the earthquake cycle. Surface-based geodetic instruments provide estimates of the overall slip distribution in larger transients but are unable to capture the detailed evolution of such slip, either in time or in space. Accompanying some of these slip transients is a relatively weak, extended duration seismic signal, known as nonvolcanic tremor, which has recently been shown to be generated by a sequence of shear failures occurring as part of the slip event. By precisely locating the tremor, we can track some features of slip evolution with unprecedented resolution. Here, we analyze two weeklong episodes of tremor and slow slip in western Shikoku, Japan. We find that these slip transients do not evolve in a smooth and steady fashion but contain numerous subevents of smaller size and shorter duration. In addition to along-strike migration rates of  $\sim 10$  km/d observed previously, much faster migration also occurs, usually in the slab dip direction, at rates of 25–150 km/h over distances of up to  $\sim 20$  km. We observe such migration episodes in both the updip and downdip directions. These episodes may be most common on certain portions of the plate boundary that generate strong tremor in intermittent bursts. The surrounding regions of the fault may slip more continuously, driving these stronger patches to repeated failures. Tremor activity has a strong tidal periodicity, possibly reflecting the modulation of slow slip velocity by tidal stresses.

**Components:** 6502 words, 19 figures, 2 animations.

**Keywords:** tremor; transient slip; Japan; subduction.

**Index Terms:** 1207 Geodesy and Gravity: Transient deformation (6924, 7230, 7240); 7240 Seismology: Subduction zones (1207, 1219, 1240); 7230 Seismology: Seismicity and tectonics (1207, 1217, 1240, 1242).

**Received** 21 March 2007; **Revised** 25 June 2007; **Accepted** 26 July 2007; **Published** 30 October 2007.

Shelly, D. R., G. C. Beroza, and S. Ide (2007), Complex evolution of transient slip derived from precise tremor locations in western Shikoku, Japan, *Geochem. Geophys. Geosyst.*, 8, Q10014, doi:10.1029/2007GC001640.

## 1. Introduction

[2] In recent years, advances in geodetic monitoring systems have led to the discovery of transient slip events in subduction zones, with durations

ranging from days to years [Hirose *et al.*, 1999; Dragert *et al.*, 2001; Ozawa *et al.*, 2002]. With similar advances in seismic monitoring networks, a weak semi-continuous seismic signal, termed non-volcanic tremor, was discovered [Obara, 2002] and

found to accompany some events on the shorter end of this duration range (days to weeks), with its activity approximately matching the duration and location of the slip event [Rogers and Dragert, 2003; Obara *et al.*, 2004]. Such “episodic tremor and slip” (ETS) events have been verified to occur in both the Cascadia and southwest Japan subduction zones. In each location, tremor and slip is concentrated downdip of the main seismogenic zone in a region believed to be transitional between velocity weakening (stick-slip) behavior updip and velocity strengthening (stable sliding) downdip.

[3] Initially, a variety of mechanisms were proposed to explain the tremor signal, often invoking fluid flow as the tremor generating mechanism [Obara, 2002; Katsumata and Kamaya, 2003; Seno and Yamasaki, 2003]. Such a mechanism arose from analogies with volcanic tremor, which is thought to be generated by the movement of volcanic fluids and from the fact that fluids are expected to be liberated from the subducting slab near where the tremor is occurring.

[4] More recently, precise locations of relatively distinct and energetic portions of tremor, classified as low-frequency earthquakes (LFEs), revealed that these LFEs occurred on the plate interface, coincident with the estimated zone of slow slip [Shelly *et al.*, 2006]. On the basis of the LFE locations and the character of their waveforms, the authors of this study proposed that LFEs may be generated directly by shear slip as part of the slip transients. This interpretation is supported by Ide *et al.* [2007a], who used stacked LFE waveforms to constrain the LFE’s mechanism. They found that LFE *P*-wave first motions and an empirical moment tensor inversion using LFE *S*-waves both yielded mechanisms supporting shear slip on the plate interface in the direction of plate convergence. Subsequently, Shelly *et al.* [2007] demonstrated that tremor could be explained as a swarm-like sequence of LFEs occurring on the plate interface. This study established that tremor itself is generated by shear slip on the plate interface and in doing so demonstrated a method to locate much of the tremor activity with high precision.

[5] An intriguing type of slip event was recently discovered to occur coincident with ETS activity in southwest Japan. These events, called very low frequency (VLF) earthquakes, are detected in broadband data at periods of 20–50 s [Ito *et al.*, 2007]. They also have mechanisms consistent with shear slip in the plate convergence direction, and

are intermediate between slow slip events and LFEs, both in duration and in magnitude.

[6] We now recognize that tremor/LFEs, VLFs, and slow slip events are all members of a family of slow shear slip events occurring together in the transition zone on the subduction interface, downdip of the seismogenic zone [Ide *et al.*, 2007b]. This slow earthquake family appears to exhibit scaling of moment ( $M_0$ ) linearly proportional to duration ( $T$ ), with  $M_0/T = 10^n$  N-m/s, where  $n$  is between 12 and 13 [Ide *et al.*, 2007b]. This is quite unlike regular earthquakes, for which moment is proportional to the duration cubed.

[7] The understanding of tremor as a direct signature of plate convergence slip allows us to use precise tremor locations to examine the evolution of slow slip events. Although geodetic measurements can resolve average properties of larger slow slip events, they cannot provide information on detailed temporal or spatial evolution of slip. Because of this, the slip in these events has often been assumed to evolve in a relatively steady fashion. We find that in western Shikoku, slow slip is a complex occurrence, likely influenced by variable frictional properties on the plate interface. Precise tremor locations give us the ability to resolve slip on a time scale of seconds, rather than days, and a spatial scale as small as  $\sim 1$  km, rather than 10 s of kilometers. Although we are limited by the locations of our LFE template sources, we can locate tremor (and thus slip) in these zones very precisely and can infer the behavior of surrounding regions. Such information could greatly assist our understanding of the physical processes controlling slow slip.

## 2. Methods

[8] In this study, we use the method described by Shelly *et al.* [2007] to examine the detailed evolution of slip during two, weeklong ETS episodes in western Shikoku that occurred during January and April 2006. This method uses the waveforms of previously located LFEs [Shelly *et al.*, 2006] as “template events” and systematically searches continuous tremor for instances where the tremor waveforms strongly resemble the waveforms of a previously recorded LFE. The similarity is measured by the sum of the correlation coefficients across all available channels of data. By utilizing multiple stations and components in the network simultaneously, this matched-filter approach becomes extremely powerful for detecting a known signal

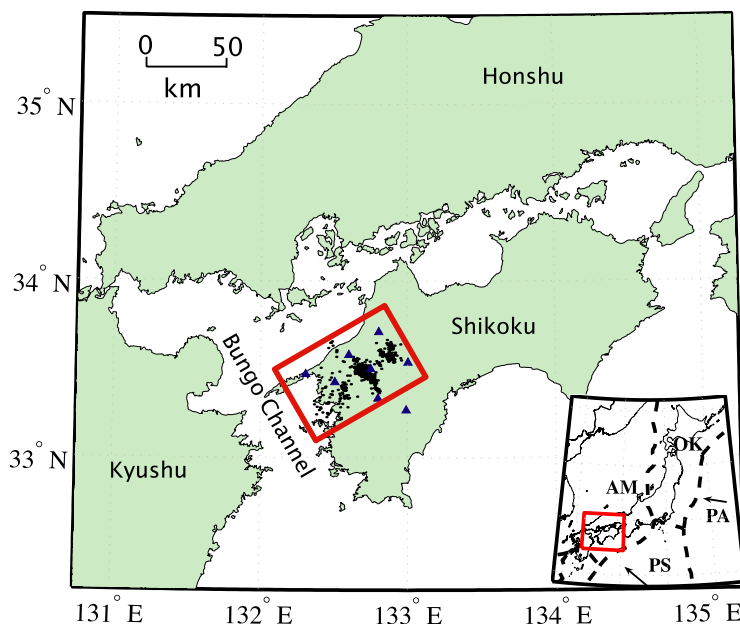


**Figure 1.** Tectonic setting and location of study area. Red box in main figure shows location of study area and denotes the region shown in Figures 3–16, parts a and b. Black dots indicate LFE template events. Blue triangles show the locations of the eight Hi-net stations used in this study. Inset shows the regional tectonics with the red box indicating the region shown in the main figure. Dashed lines indicate approximate plate boundaries. PA, Pacific plate; PS, Philippine Sea plate; AM, Amur plate; OK, Okhotsk plate.

in noisy data, while minimizing false detections [Gibbons and Ringdal, 2006; Shelly *et al.*, 2007].

[9] For this study, we use continuous data from eight, three-component Hi-net stations in western Shikoku. As done by Shelly *et al.* [2007], we select template LFEs based on the number of stations recording the event. In this case, we select each LFE [Shelly *et al.*, 2006] recorded by at least five of the eight stations, giving a minimum of 15 channels of data for each template event. This selection criterion gives 609 LFE template events and ensures both that these are well located and that they have sufficient data to allow detection of similar events within the continuous tremor waveforms.

[10] As done by Shelly *et al.* [2007], we adopt a detection threshold based on the median absolute deviation (MAD) of the distribution of correlation sums. Our detection threshold is set at  $8 \times \text{MAD}$  and is set independently for each template event and each day of continuous seismic data. At this threshold, on the basis of statistical arguments supported by synthetic tests [Shelly *et al.*, 2007], we estimate the false detection rate to be about 1 per hour (total over all 609 template events). Sometimes, we consider a “very robust” detection threshold of  $9 \times \text{MAD}$ . This very high detection threshold (probability of exceedance of  $\sim 6.4 \times 10^{-10}$

for a Gaussian distribution) sacrifices a large number of legitimate detections but virtually eliminates spurious detections. In other words, we are willing to accept a large number of type II errors to minimize the number of type I errors. With this detection threshold, we expect our false detection rate to be less than one event per day. For either threshold level, we assign a detected event to the location of the template event with the strongest detection in each 2-s window [Shelly *et al.*, 2007].

### 3. Results and Discussion

[11] We examine two ETS episodes occurring in western Shikoku during January and April 2006. Figure 1 shows the regional tectonics and location of our study area, as well as the epicenters of our template LFEs. Tilt data and the associated slip model for the April event, as determined by Sekine and Obara [2006], are shown in Figure 2. For this event, they estimate a moment magnitude  $M_w = 6.0$ , and an average of 1.2 cm of slip, based on the tilt change at multiple stations during a three-day period from 17–20 April. No geodetic-based slip model is currently available for the January event, as it apparently did not generate a sufficient tilt signal to enable modeling of a fault plane. This may be due to the fact that, based on our tremor locations, the January 2006 event ruptured a smaller

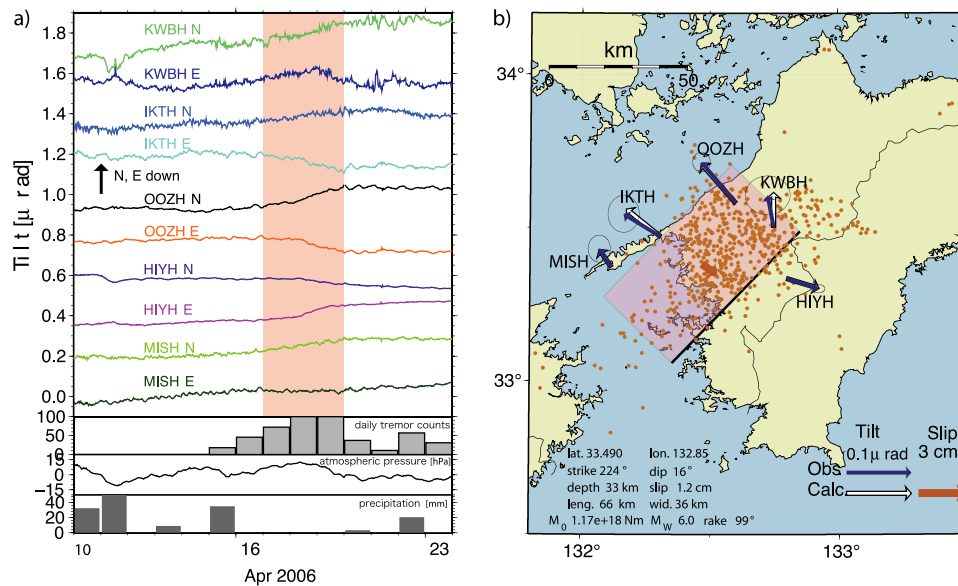


**Figure 2.** The April 2006 tremor and slip event. (a) From top to bottom: time series of tiltmeter records, daily tremor counts, atmospheric pressure, and precipitation from 10–24 April 2006. Station names and components are given next to each tiltmeter record. The records are plotted after removing their linear trend and estimated tidal and atmospheric components (figure from *Sekine and Obara* [2006]). (b) Tilt change vectors (blue arrows; ground downward direction), the estimated short-term slow slip model (red rectangle area and arrow) from these tilt change data, and the calculated tilt changes due to this short-term slow slip event model (open arrows) for the western Shikoku region. Epicenters of deep low-frequency tremor activity are also plotted during the same time period (17–20 April 2006) (figure from *Sekine and Obara* [2006]).

area than the April event, extending a shorter distance to the southwest (see Figures 3–16).

[12] Figures 3–9 and 10–16 demonstrate the complex evolution of tremor and slip during the episodes of 15–21 January and 15–21 April 2006, respectively, based on precise tremor locations. Figure 17 shows a zoom of four prominent migration episodes from Figures 3–16. For a different perspective on these episodes, please see Animations 1 and 2. In total, we detect 7,297 events during the January episode and 3829 events during the April episode. Of these, 3924 and 1905 events in January and April, respectively, correspond to “very robust” detections, exceeding the threshold of  $9 \times \text{MAD}$  (see methods). Since these events have been shown to represent shear failure on the plate interface, we believe the locations accurately reflect portions of the plate boundary slipping at any given time. Although potential locations are limited to places where we have LFE template sources (Figures 3–16), we can use these locations to infer the behavior of the surrounding region as well. In fact, the locations of the template LFEs themselves with their often-clustered distribution may contain information about the properties of the plate boundary.

[13] One of the characteristics obvious from Figures 3–16 is the repeated tremor (and thus slip) activity on portions of the plate interface covered by template LFEs during a given ETS episode. The repeat time of such ruptures is not regular but may be related to stresses resulting from slip on neighboring portions of the fault. Such episodes often appear to rupture the fault through an entire template LFE cluster, but individual clusters rupture more or less independently. Even closely spaced “subclusters” of template LFEs in the northeast part of our study area (along-strike position  $\sim 60$  km) often display bursts out of phase from one another, while concurrently active in general. This behavior suggests a scenario where the fault at these template LFE clusters is driven to failure by steadier slip on the surrounding portions of the fault. These LFE cluster zones may be places on the plate interface with frictional properties different from those of the surrounding material, or they may represent some sort of geometrical heterogeneity. Under this scenario, these cluster zones may be analogous to repeating earthquake patches, which are believed to be portions of the fault that exhibit unstable slip surrounded by a stably slipping region [e.g., *Schaff et al.*, 1998]. As in

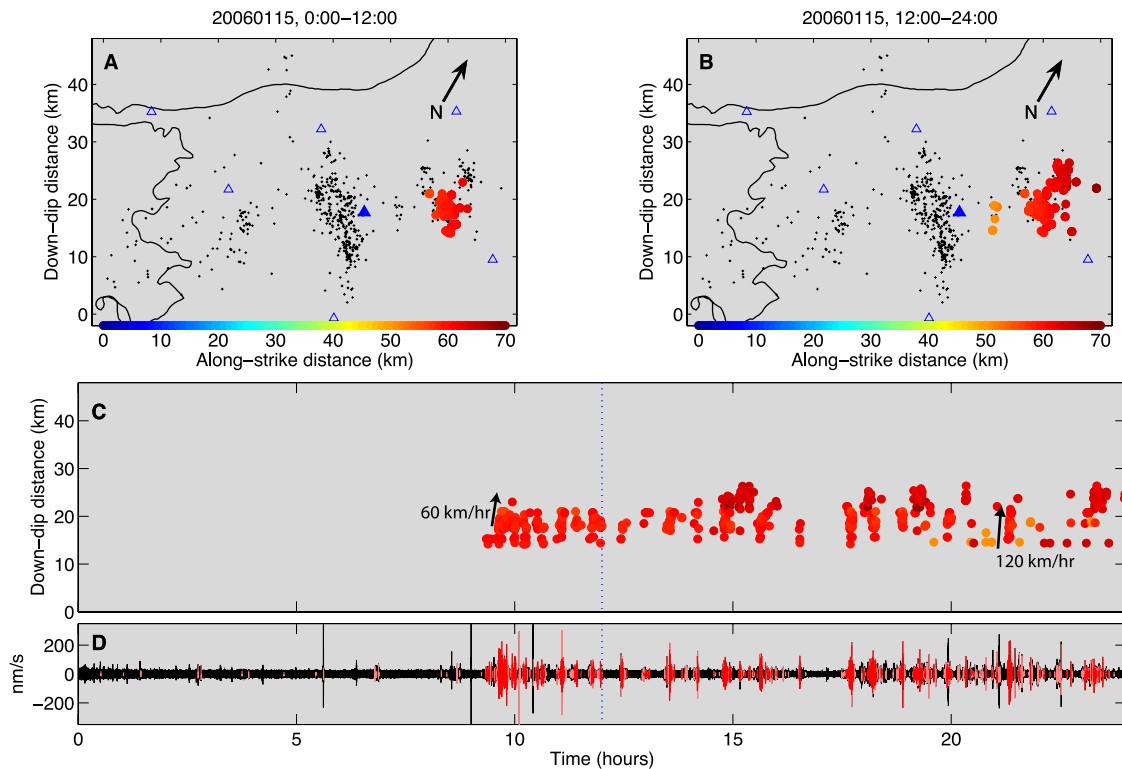


**Figure 3.** Figures 3–9 show the space-time progression of tremor during 15–21 January 2006. Date is given by figure heading. (a) Map view showing active LFE template events (colored circles) during the first half of each day (0000–1200 LT). The color scale indicates the along-strike position, for reference when comparing with Figure 3c. Only very robust detections exceeding  $9^*MAD$  (see text) are plotted. If multiple detections are present, the strongest in each 2-s window is plotted. Black dots show epicentral locations for LFE template sources. Blue triangles indicate the locations of Hi-net stations used in this study, with the solid triangle showing station N.KWBH referred to in Figure 3d. The black line is the coastline of Shikoku. (b) Same as Figure 3a, but for the second half of each day (1200–2400 LT). (c) Down-dip position of tremor versus time. Events are color-coded by along-strike position as in Figures 3a and 3b. Arrows and labels indicate the direction and approximate migration velocity for some of the clearest examples of migration, as determined by visual inspection of a zoomed view. Notice the migration of tremor that can be seen in both the updip or down-dip directions. Black boxes indicate the times and locations of zoomed views in Figure 17. (d) Seismic waveform from station N.KWBH, north component (location shown in Figure 3a). Portions of the waveform plotted in red indicate times of very robust detections (exceeding  $9^*MAD$ ), while portions plotted in pink indicate times with standard detections (exceeding  $8^*MAD$ ; see text for details). A relatively steady, low-amplitude signal seen around midday and uncorrelated with LFEs does not appear to be nonvolcanic tremor, as neighboring stations do not record a similar signal.

the case of repeating earthquakes, the repeat time of rupture may be related to slip rates in the surrounding region [Nadeau and McEvilly, 1999]. Slip episodes across LFE cluster zones, however, proceed over a matter of minutes, rather than seconds as for earthquakes of comparable rupture dimension.

### 3.1. Migration of Tremor and Slip

[14] We observe two classes of migration of ETS activity: a relatively slow migration along-strike and a much faster migration usually observed in the dip direction of subduction. Previous investigators have observed that ETS episodes often

exhibit along-strike migration rates of approximately 5–20 km/d [Obara, 2002; Dragert *et al.*, 2004; Kao *et al.*, 2006]. Kao *et al.* [2007] described some variations on this behavior including pauses in tremor migration (“halting”) and “jumps” in active zones from one place to another. We observe similar, sometimes unsteady, migration trends in both the January and April events. In January the along-strike migration is mostly unilateral, whereas in April migration occurs bilaterally. Superimposed on this slow average migration, however, is a much more complex short-term behavior, where we observe portions of the fault that generate strong tremor (LFEs) rupturing repeatedly.

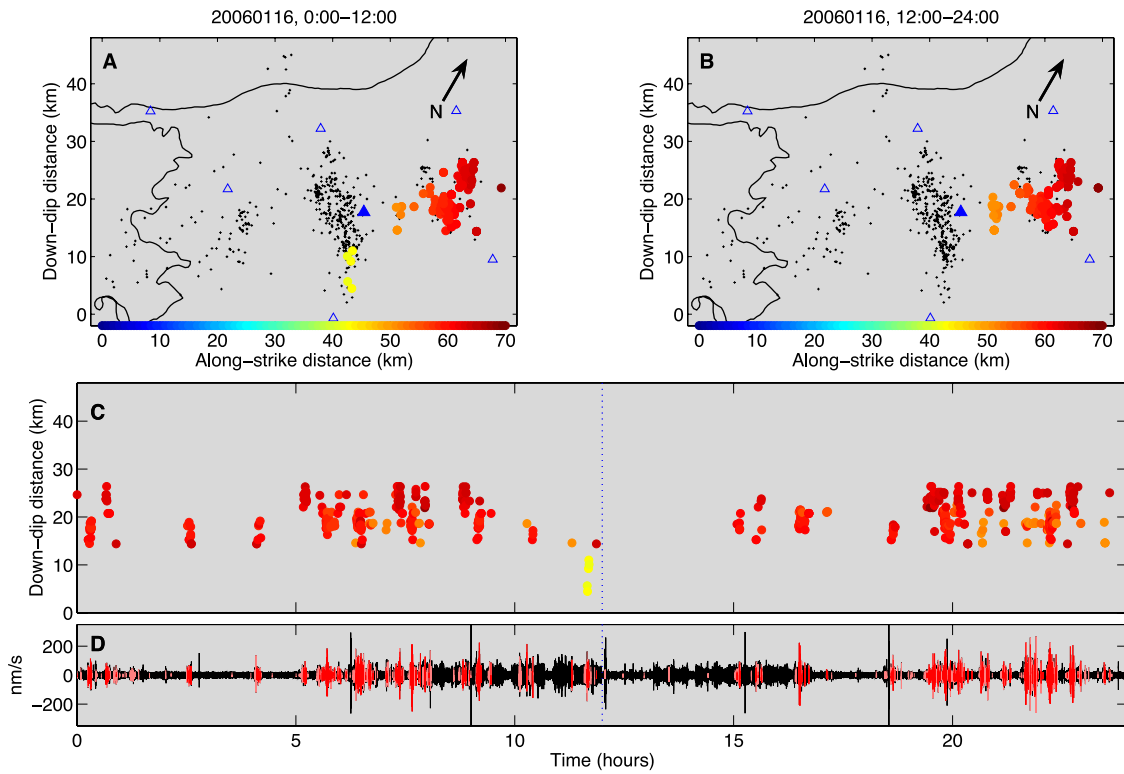


Figure 4. Same as Figure 3, but for 16 January 2006.

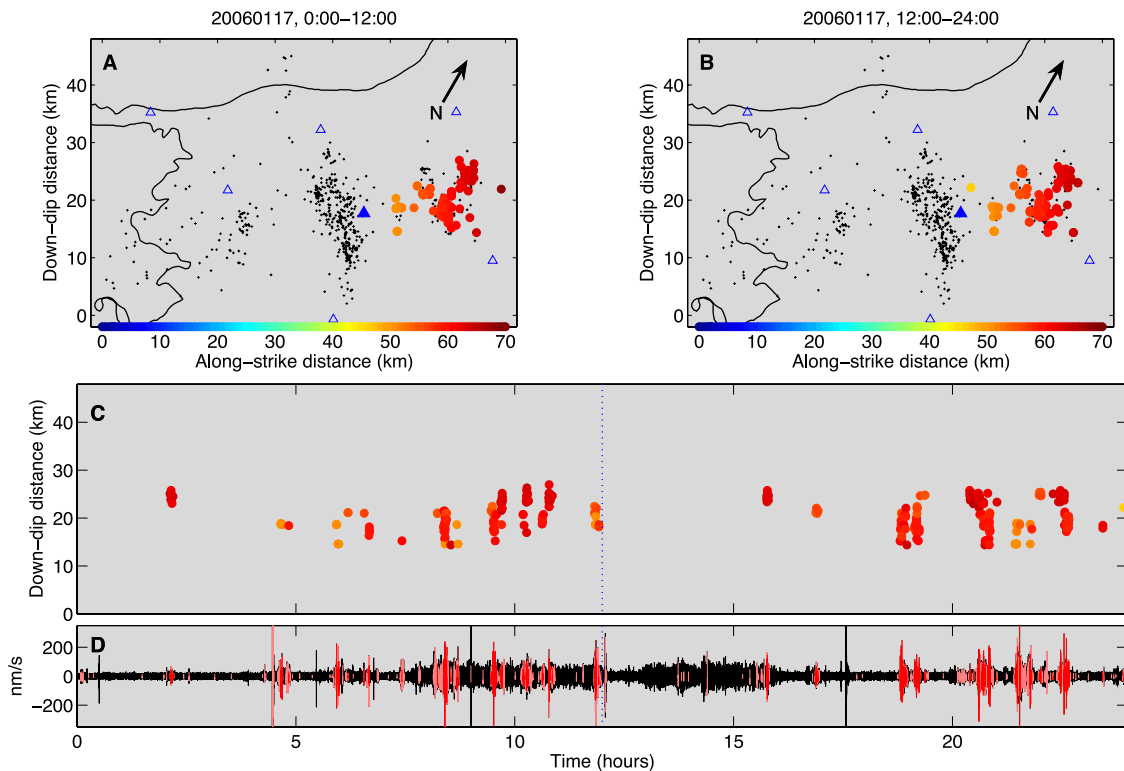
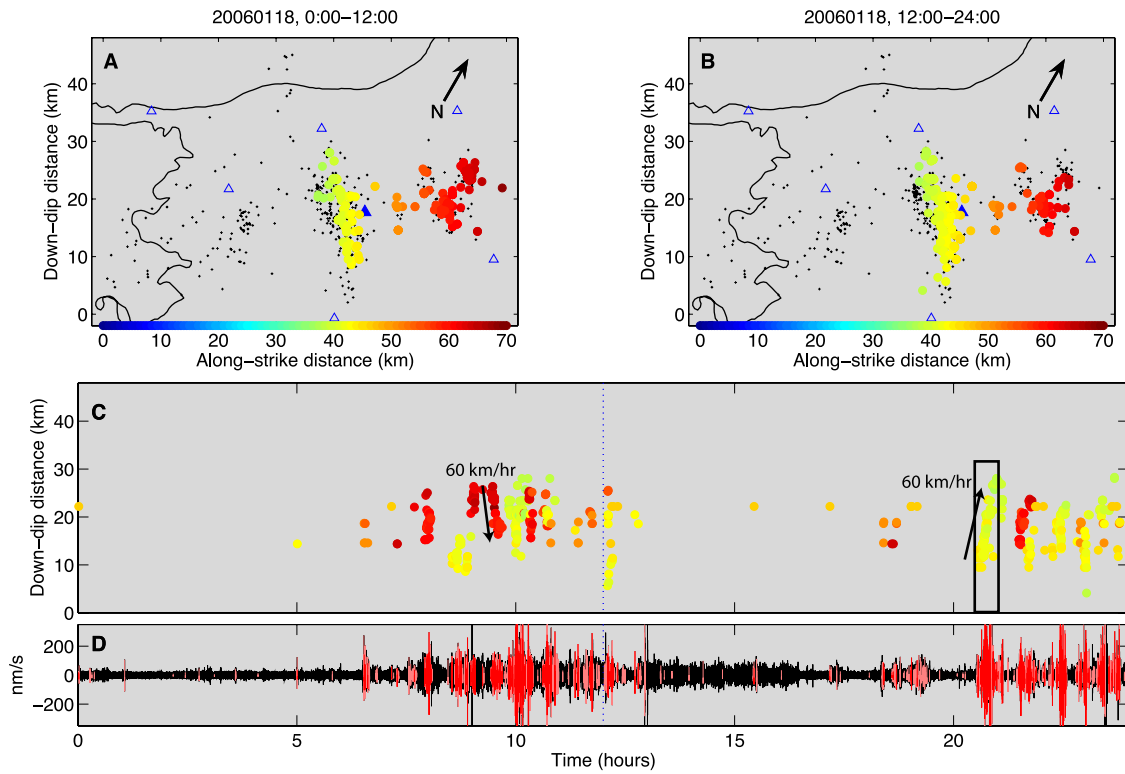
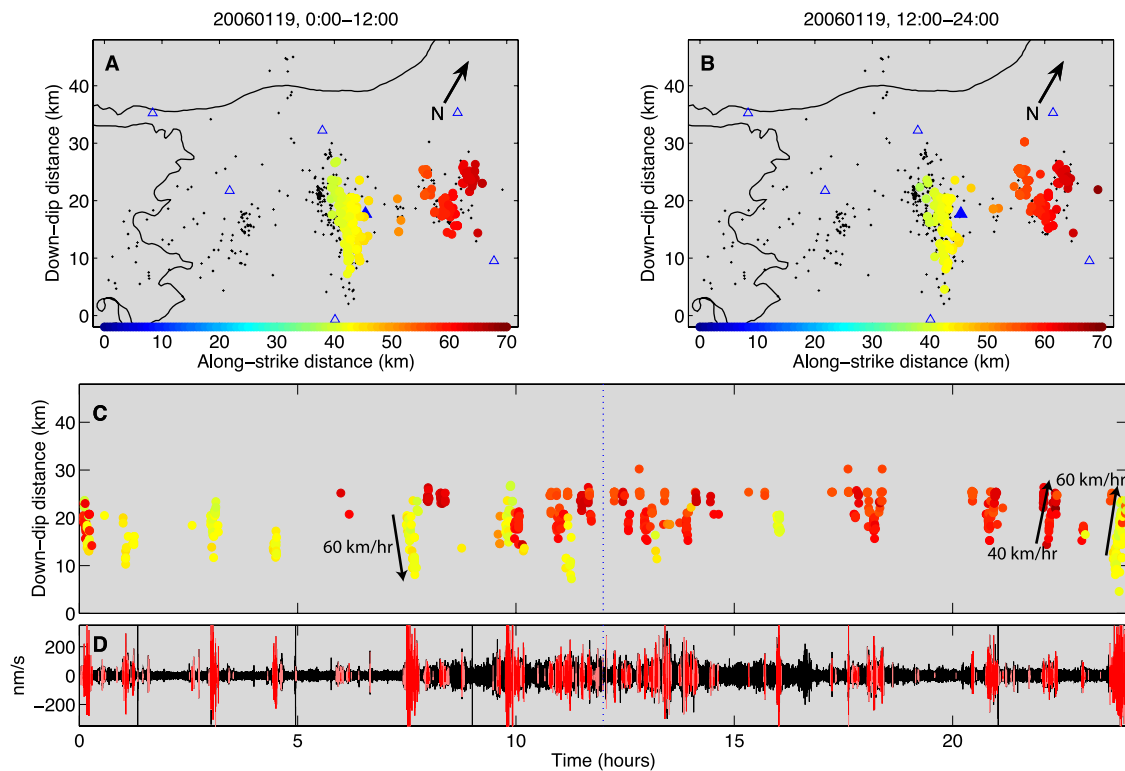


Figure 5. Same as Figure 3, but for 17 January 2006.



**Figure 6.** Same as Figure 3, but for 18 January 2006.



**Figure 7.** Same as Figure 3, but for 19 January 2006.

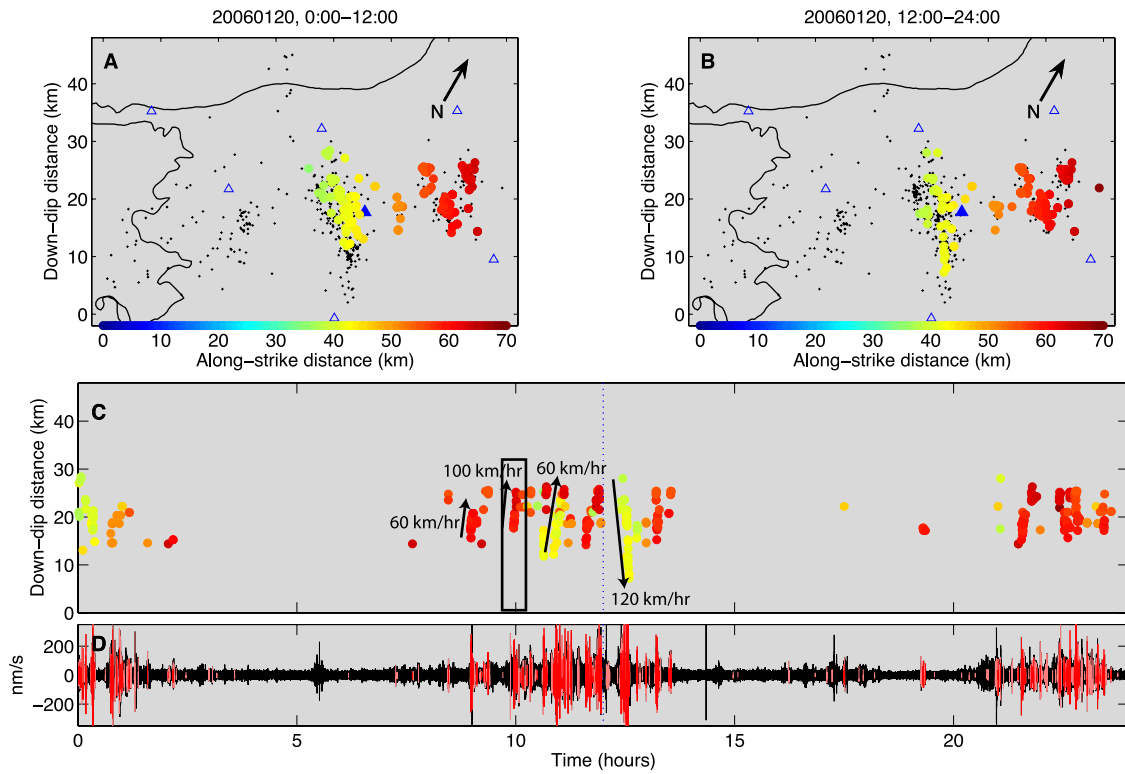


**Figure 8.** Same as Figure 3, but for 20 January 2006.

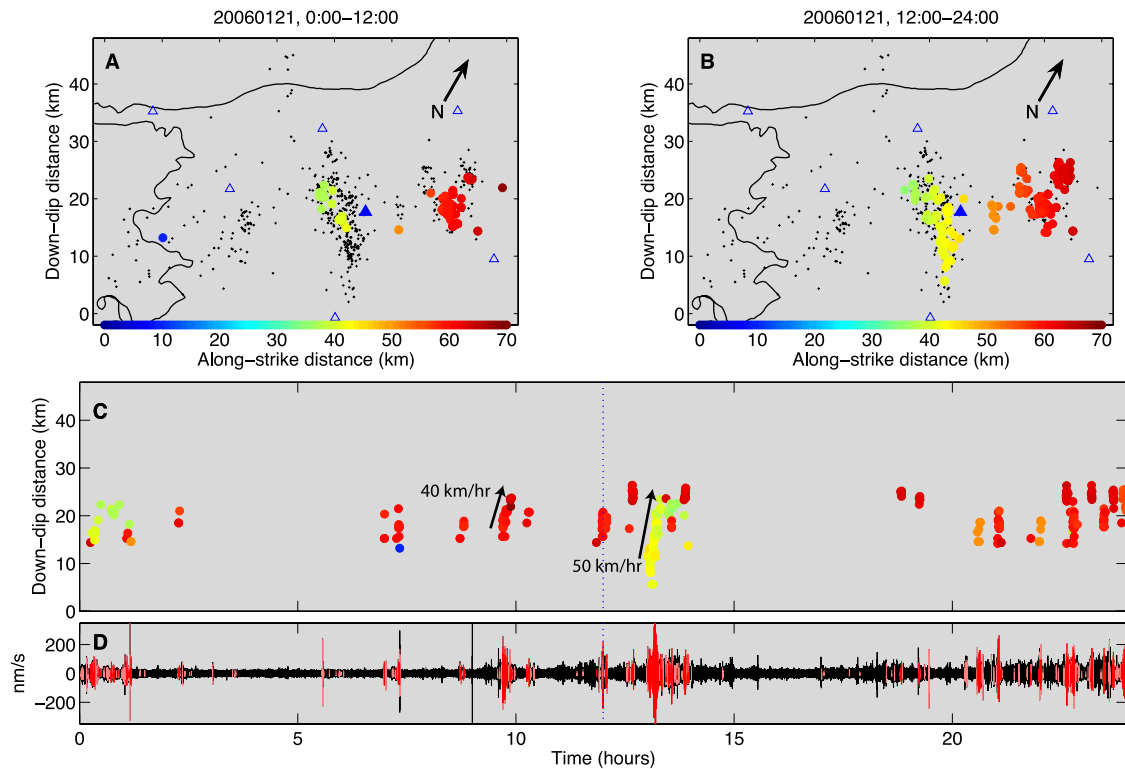


**Figure 9.** Same as Figure 3, but for 21 January 2006.

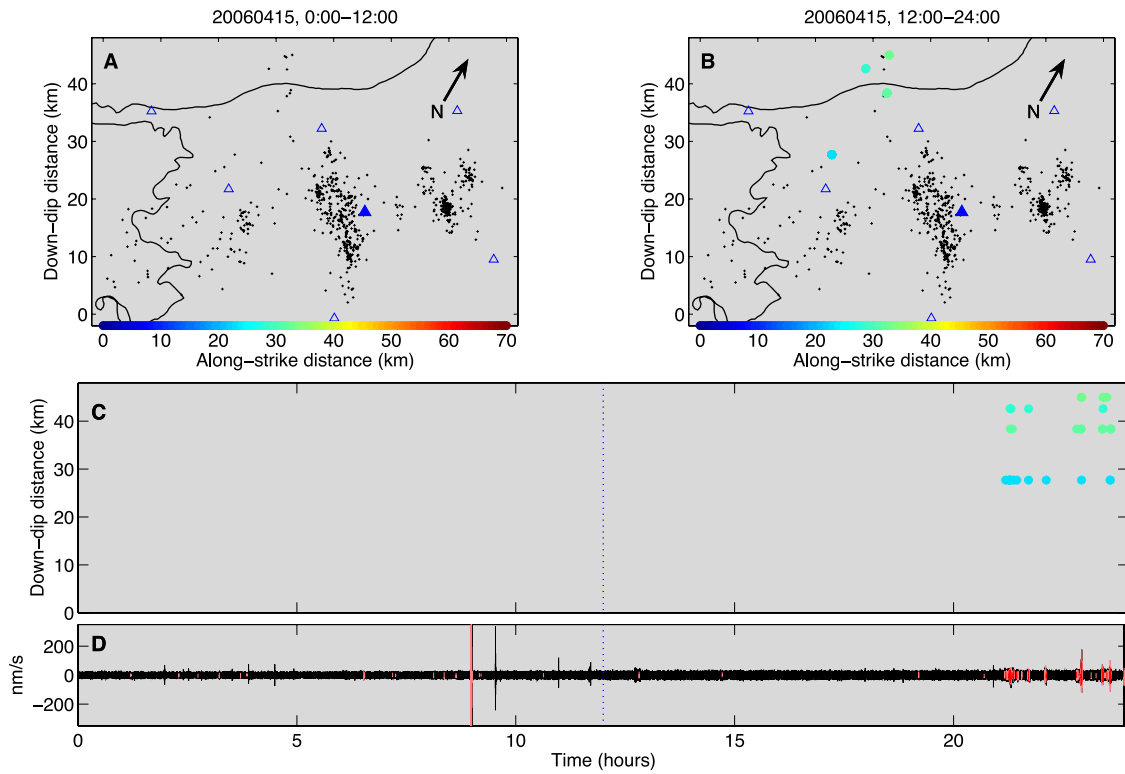


Figure 10. Figures 10–16 are the same as Figures 3–9, but for 15–21 April 2006.

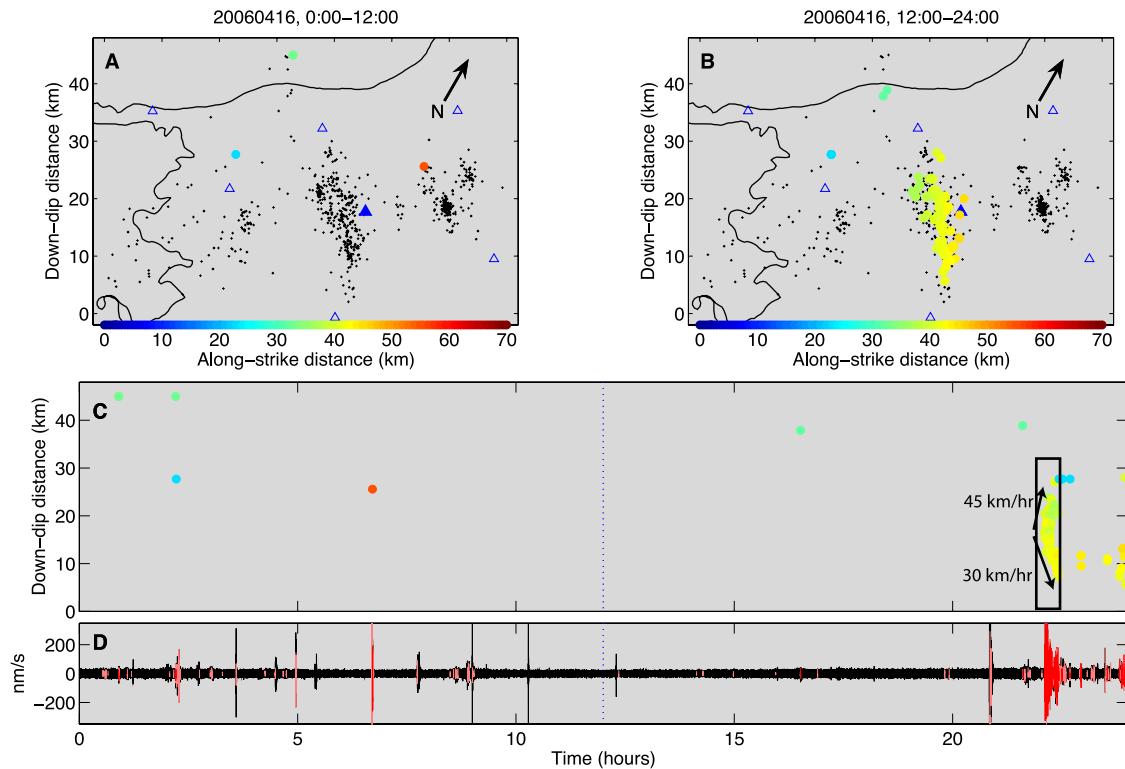
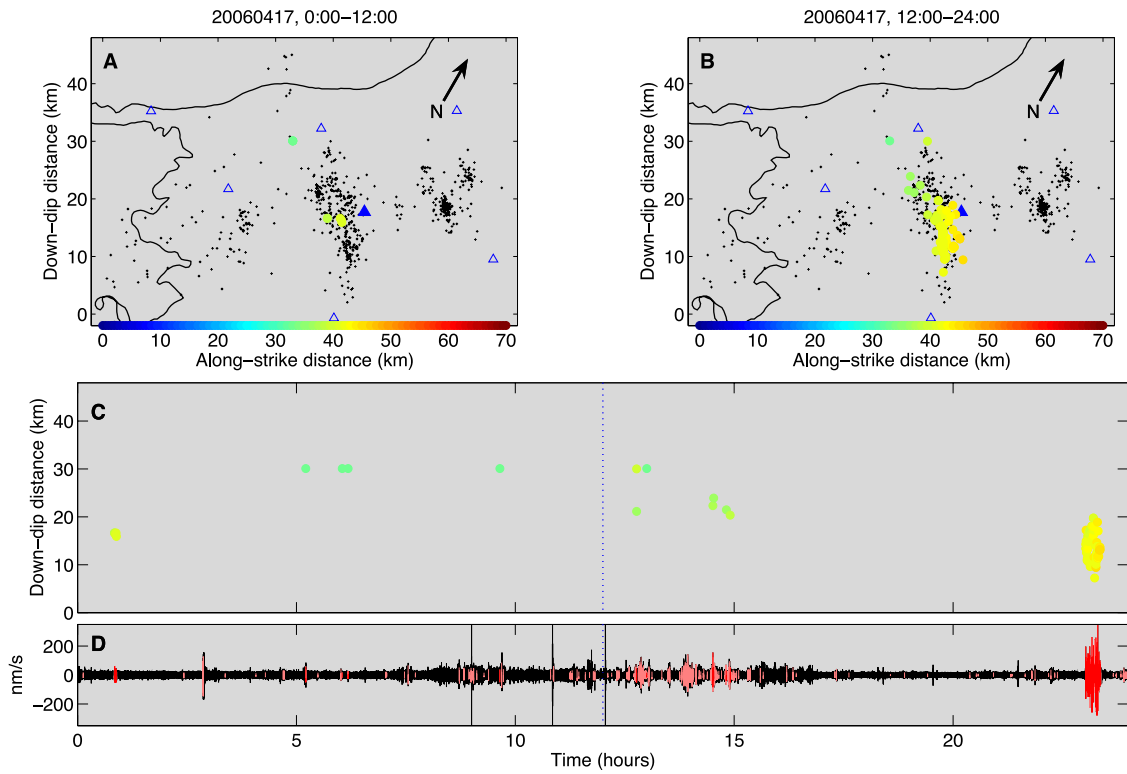
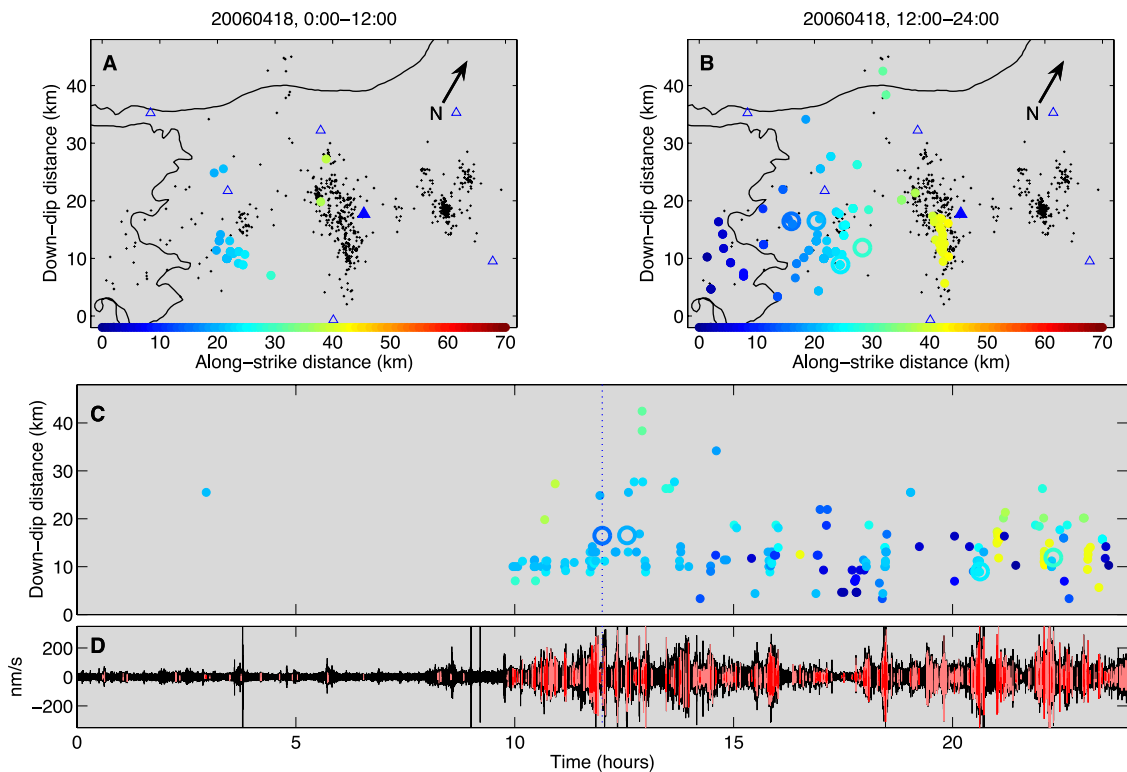


Figure 11. Same as Figure 10, but for 16 April 2006.



**Figure 12.** Same as Figure 10, but for 17 April 2006.



**Figure 13.** Same as Figure 10, but for 18 April 2006. Large open circles in Figures 13b and 13c indicate the occurrence of VLF events, as reported by *Ito et al.* [2007].

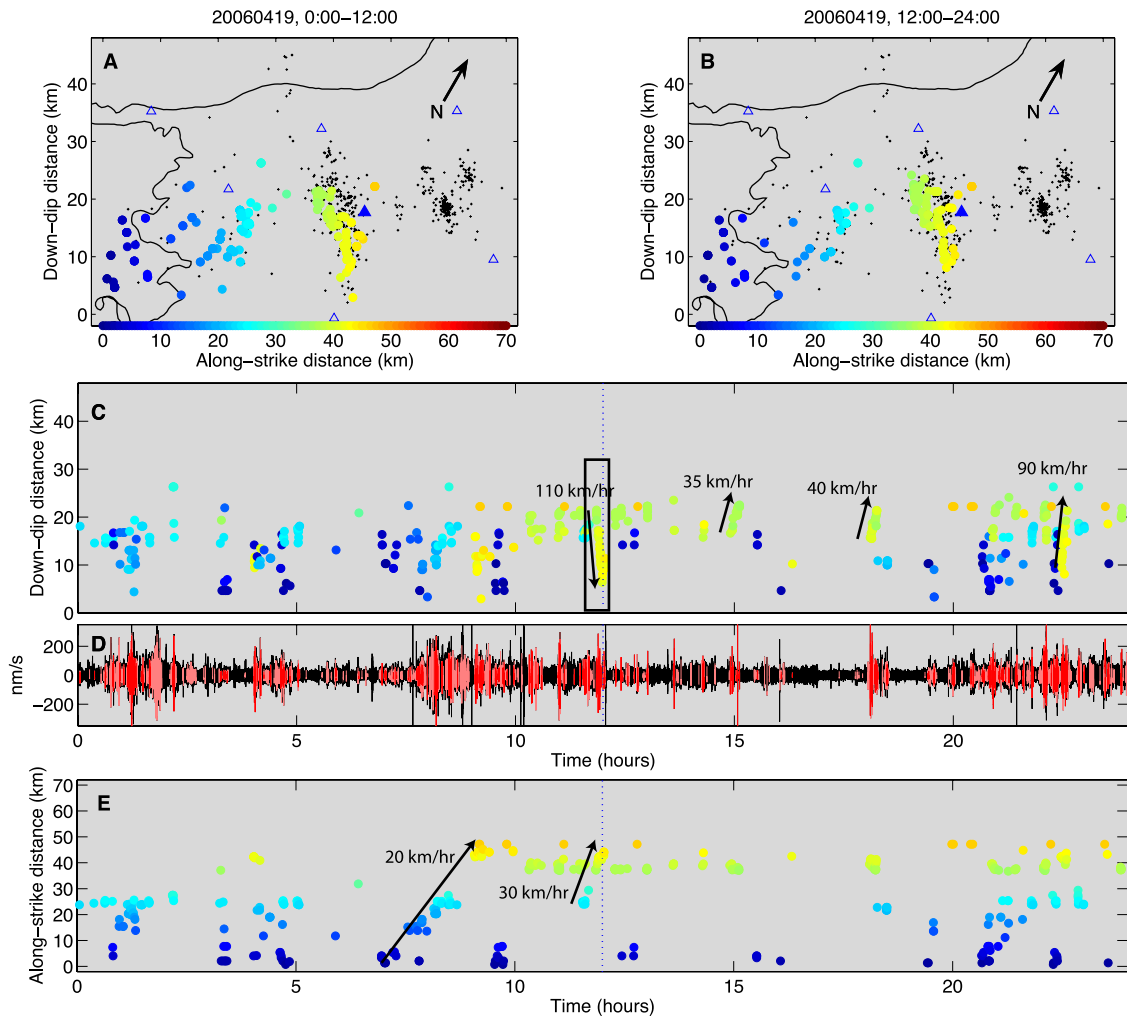


**Figure 14.** Same as Figure 10, but for 19 April 2006. Figure 14e shows the along-strike position of tremor versus time.

[15] Using precise tremor locations, we can resolve much higher rates of migration of tremor and slip than has previously been possible. The clearest of these migrations occur in approximately the dip direction at  $\sim 20\text{--}150$  km/h, as highlighted in Figures 3–16. Occasionally, migration at similar rates can also be seen in the along-strike direction. These rates are 40–300 times faster than a typical long-term along-strike migration rate of  $\sim 12$  km/d. However, they are still approximately 3 orders of magnitude slower than ordinary earthquake rupture velocities. These migrations are easiest to observe in the LFE cluster located at an along-strike position of  $\sim 40$  km, where rupture commonly propagates  $\sim 15$  km along-dip in  $\sim 15$  min. If these events do not extend significantly beyond our template LFEs and the scaling relationship proposed by *Ide et al.* [2007b] is applicable, such episodes would be expected to have a moment

magnitude of approximately  $M_w = 4.3$ , falling between VLF events and slow slip events in size and duration.

[16] Most of the clear migration episodes occur in the updip or downdip direction. The clusters of template LFEs tend to be extended in the dip direction, but narrow along strike, raising the possibility that the migration velocities we observe are apparent, rather than true velocities. Apparent velocity will always be higher than true velocity, but the high velocities we observe in these episodes cannot be explained away as due to apparent velocities for several reasons.

[17] First, the observed velocities fall in a narrow range. If the migration directions were random, we would observe a wide range of apparent velocities. The apparent velocity varies as the secant of the angle between the seismicity distribution and the

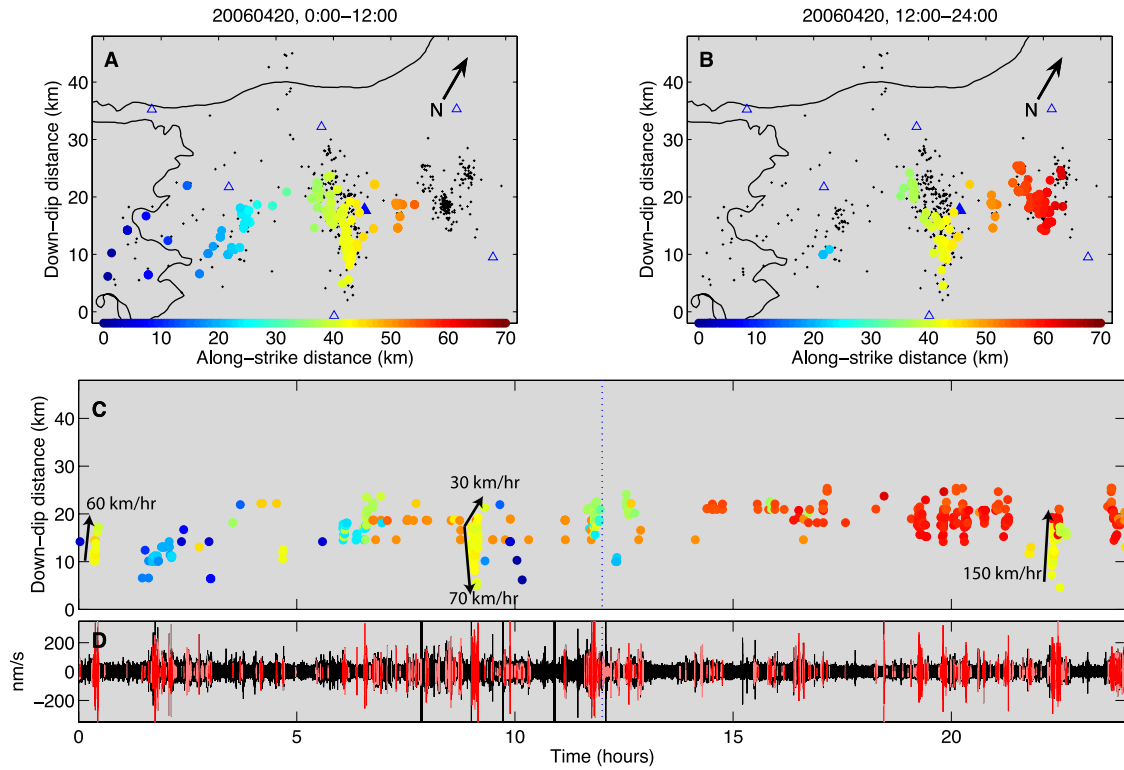


Figure 15. Same as Figure 10, but for 20 April 2006.

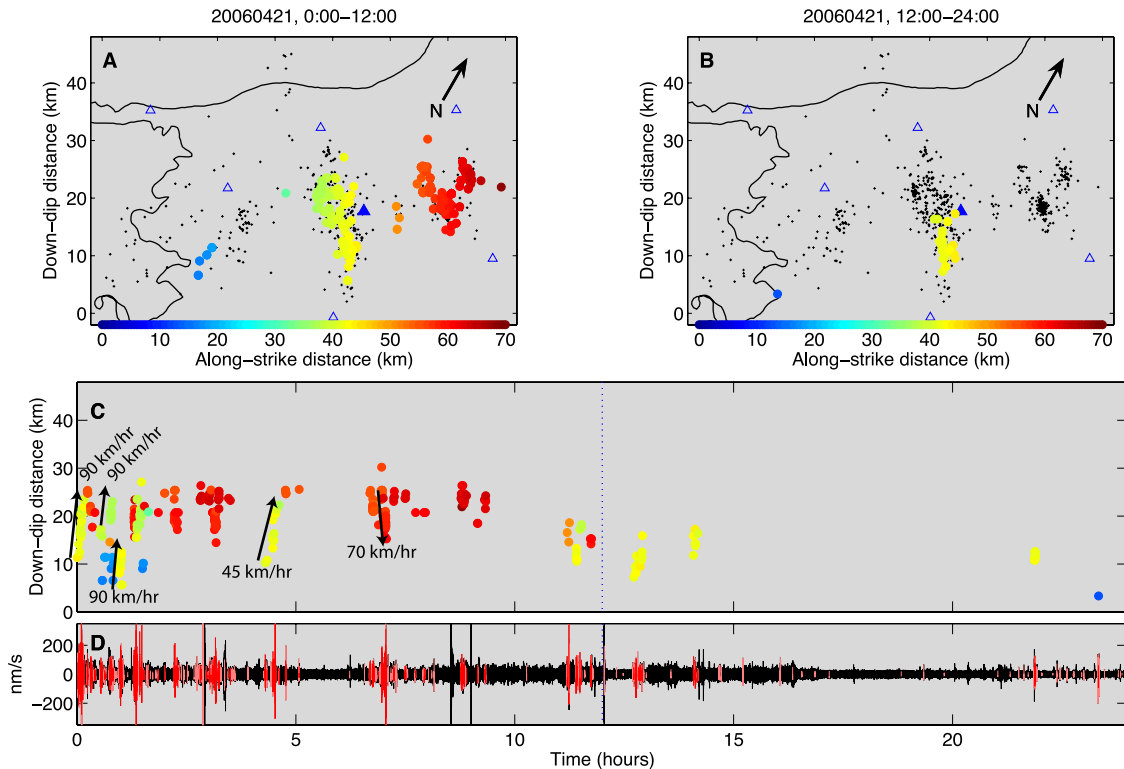
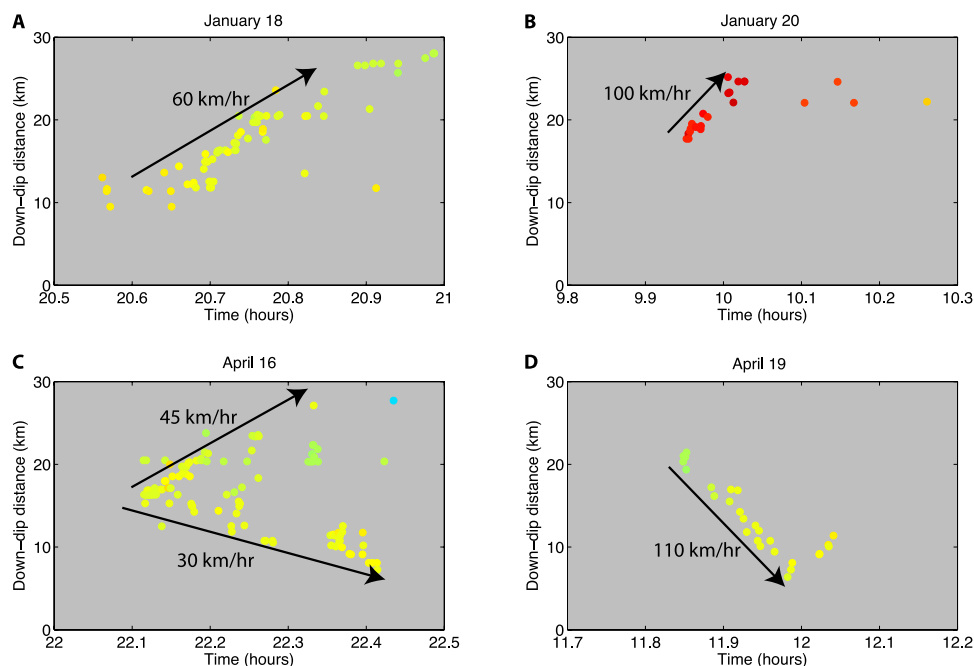


Figure 16. Same as Figure 10, but for 21 April 2006.



**Figure 17.** Zoomed view of four migration episodes, plotted as down-dip distance versus time. Each panel shows a 30-min period: (a) 18 January (Figure 6), (b) 20 January (Figure 8), (c) 16 April (Figure 11), and (d) 19 April (Figure 14). These panels demonstrate the variety of migration modes, including updip (Figure 17d), downdip (Figures 17a and 17b), and bilateral (Figure 17c).

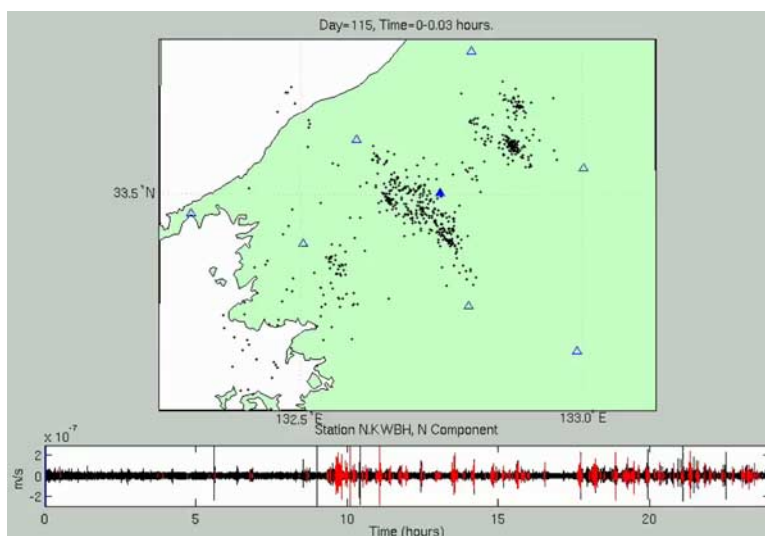
direction of the true velocity. In order to have an apparent velocity that is an order of magnitude higher than the true velocity, this angle would have to be less than  $\sim 5^\circ$  for each episode. Second, we can resolve migration in both strike and dip direction quite well for a substantial portion of our study region, including the area with an along-strike position of 35–65 km. In this region, although we have sufficient resolution, we do not observe a corresponding slower migration in the along-strike direction, as would be expected if we were measuring the apparent velocity. Finally, the migrations seen repeatedly in the same areas preclude a model where one simple slip pulse migrates at a few km/d in the along-strike direction. For all of these reasons we believe that the velocities we observe are representative of the true, rather than apparent, migration velocities.

[18] In different along-dip episodes, the migration direction can be updip, downdip, or bilateral. The downdip migration examples, combined with very high migration rates, make it unlikely that fluids migrate with this slip. Instead, the events are most likely triggered by a combination of stresses accumulating from slower, steadier slip on surrounding regions of the fault and the stresses induced by adjacent LFEs within a migration sequence. This

larger-scale, more-continuous slip appears to grow slowly in size, controlling the overall along-strike migration, while the smaller-scale events grow much more quickly, consistent with the scaling relationship proposed by *Ide et al.* [2007b].

[19] We rarely observe clear examples of fast migration along strike. Although gaps in our distribution of template LFEs may render it difficult to recognize along-strike migration if it propagates for less than 10 km, we can conclude that larger-scale episodes are rare. For example, ruptures propagate up to 20 km along dip through the large LFE cluster near the center of our study area (along-strike position of  $\sim 40$  km) without propagating to separate LFE clusters within 10 km along strike.

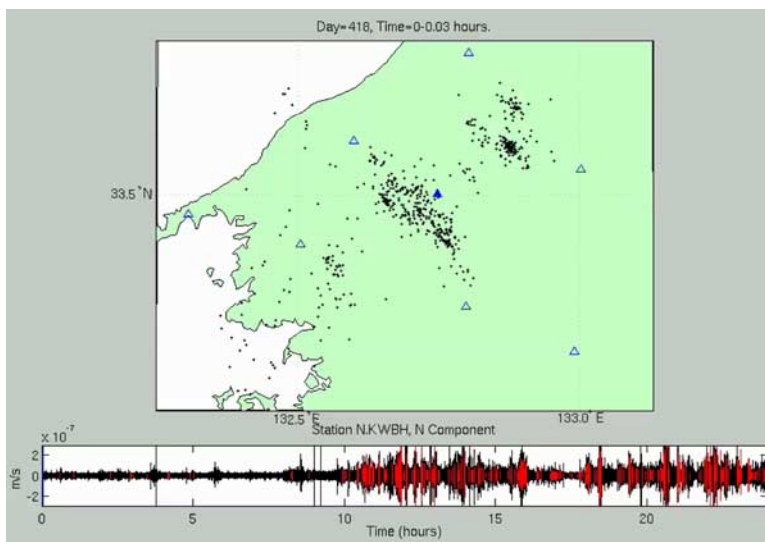
[20] A notable exception occurred on 19 April 2006 and is shown in Figure 14e. This particular example migrates to the northeast 50 km along strike over a period of 2.5 hours, an average rate of 20 km/h. If this episode did not extend significantly outside our study region, the scaling relationship of *Ide et al.* [2007b] would suggest a magnitude near  $M_w = 5.0$ . This fast along-strike migration episode is superimposed on top of a slowly migrating tremor front and likely represents a propagating pulse of faster slip within the larger transient slip



**Animation 1.** Animation showing detected events with time during nonvolcanic tremor for 7 days, 15–21 January 2006. (top) Map view of western Shikoku region. Template events are plotted as small black crosses. Colored circles represent a detected event, using the normal threshold of 8 times the median absolute deviation of the distribution of correlation sums for each template event. The shade of the circle represents the robustness of the detection, with light orange indicating a detection just above the threshold level and bright red indicating a detection at 2 or more times the threshold. Each frame represents 2 minutes, with strongest detection from each 2-second window plotted. The symbols are plotted in reducing size and shading toward black for 3 frames beyond the detection time in order to guide the eye. Blue triangles show station locations; the filled triangle indicates the station with waveforms plotted in the bottom panel. The time listed at the top corresponds to the approximate time of the first S-wave arrival at any station. (bottom) A sample velocity waveform, one hour in duration, corresponding to the time period of the animation. Waveform is station N.KWBH, north component, band-pass filtered between 1 and 8 Hz. Portions plotted in red indicate times with a detected event similar to a template event. The vertical blue bar indicates the point in time represented in the map view. Animation available in the HTML.

event. Although the physical dimensions of the event may play a role [Ide *et al.*, 2007b], the processes controlling these two very different migration rates are not well understood. Segmen-

tation of the fault may inhibit extensive propagation of “fast” pulses of slip along strike. This segmentation could be due to small geometrical irregularities, which would be expected to align in



**Animation 2.** Same as Animation 1, but for the period from 15–21 April 2006. Animation available in the HTML.

the direction of slip (similar to the slab dip direction) forming a corrugation over time. In fact, a corrugation of the fault may also influence the distribution of LFE template sources, which are sometimes located in clusters approximately aligned with the plate convergence direction. This phenomenon could be related to streaks of seismicity aligned in the slip direction observed on creeping faults elsewhere [Rubin *et al.*, 1999; Waldhauser *et al.*, 2004]. In the case of our study area, on the basis of the propagation of tremor activity, the plate boundary appears more strongly segmented to the northeast than the northwest. Perhaps, only the larger, slower “main event” is readily capable of overcoming this segmentation.

[21] For both slow and fast migration, the onset of activity is usually much sharper than the ceasing of activity on a given portion of the fault. These trailing events could be considered “aftershocks” of the major sequence of activity; they may be due to residual stresses or simply indicate a fault weakened immediately after rupture that heals over time.

### 3.2. Relationship to Very Low Frequency Earthquakes

[22] Ito *et al.* [2007] found VLF events coincident with ETS activity in southwest Japan and identified four such events occurring as part of the ETS episodes examined here. All four occurred on 18 April 2006; their reported locations and timing relative to our tremor locations are shown by the open circles in Figure 13. The magnitudes of these four events were estimated to range from  $M_w = 3.2$  to  $M_w = 3.5$ , with durations on the order of 10 s [Ito *et al.*, 2007]. Although we clearly see tremor activity in the vicinity of the reported VLF events before and after their occurrence, such activity is unremarkable compared to other times when VLF events were not reported. The relatively small size and short duration of the VLF events combined with somewhat sparse template LFE coverage in the vicinity of the VLFs probably explain this lack of signal.

### 3.3. Tidal Triggering of Tremor and Slip

[23] Tremor activity observed in the January 2006 event exhibits a strong periodicity at slightly more than 12 hours, very similar to the average tidal period of 12.4 hours. The effect is so strong it can be seen visually in Figures 3–9 as two distinct maxima of activity each day, suggesting a much more dramatic tidal influence than that reported

for various populations of regular earthquakes [Tsuruoka *et al.*, 1995; Tanaka *et al.*, 2002; Cochran *et al.*, 2004]. Schuster’s test [Schuster, 1897] is often used to test statistical significance of tidal triggering of earthquakes [e.g., Tanaka *et al.*, 2002; Cochran *et al.*, 2004]. For each event, Schuster’s test assigns a unit vector in the direction defined by its phase angle; the phase angle in our case is related to the tidal phase. The squared length of the vectorial sum for all events,  $D^2$ , is given by

$$D^2 = \left( \sum_{i=1}^N \cos \theta_i \right)^2 + \left( \sum_{i=1}^N \sin \theta_i \right)^2$$

where  $\theta_i$  is the phase angle of the  $i$ th event and  $N$  is the total number of events. Assuming the events occur randomly and independently, the probability of obtaining a vectorial sum equal to or greater than  $D$  is

$$P = \exp\left(-\frac{D^2}{N}\right)$$

Therefore  $1-P$  represents the significance level to reject the hypothesis that the events occur randomly. Assuming a period of 12.4 hours, we obtain  $P$  values that are vanishingly small for both the January and April events. In our case, however, because of the strong clustering of events in time, their occurrence is not independent and  $P$  likely overestimates the significance.

[24] Even disregarding the absolute  $P$ -value, the tidal influence can be clearly seen by comparing the result of Schuster’s test for a range of possible periods. Figure 18 shows the results of such a “relative” Schuster’s test by plotting  $D^2/N$ , the argument of the exponential in Schuster’s test, versus tested period. For both episodes, phase angles are assigned starting with 0 and ranging to  $2\pi$ , repeating with the period to be tested. Figure 18 shows an exceptionally strong peak at just over 12 hours for the January event. The actual peak occurs near 12.3 hours, slightly shorter than an average tidal period of 12.4 hours, but consistent with the average tidal period during this particular time span, as evidenced by nearby sea-tide records. Peaks in tremor activity levels for the January event correspond to during and shortly after the high tide recorded on the Pacific coast of Shikoku. The April episode also exhibits a strong peak near a period of 12 hours, although the effect is subtler than for the January event. Figure 19 shows histograms of event abundance versus phase angle for the two episodes, assuming a period of 12.4 hours.

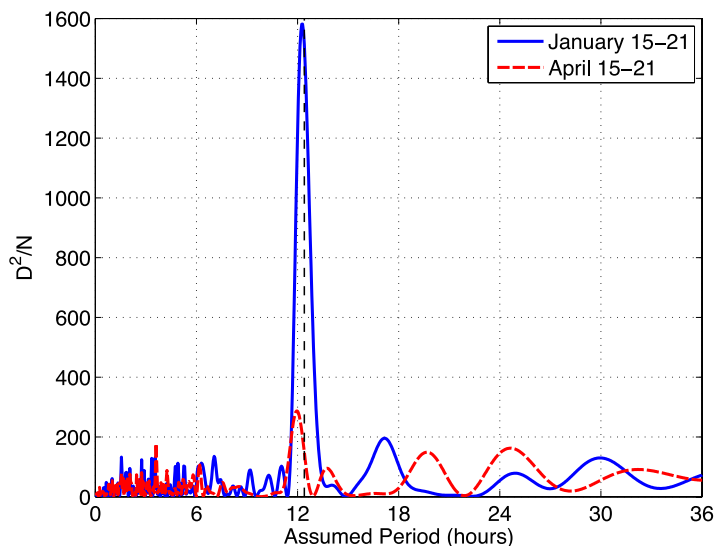


**Figure 18.** Evidence for tidal triggering of LFE activity. The population of detected LFEs during each tremor and slip episode is analyzed for nonrandomness at periods from 0.2 to 36 hours. The quantity  $D^2/N$  relates to the statistical significance of the nonrandomness in Schuster's test (see text). The January event (solid blue line) exhibits an extremely strong periodicity near the average tidal period of 12.4 hours (dashed black line). Tidal triggering in the April event (dashed red line) is less obvious, but this episode still shows a periodicity very close to the average tidal period.

[25] Although we do not attempt to calculate the tidally induced stress, previous studies have emphasized the importance (and often domination) of ocean tide loading effects relative to solid earth tides when near ocean basins [Tsuruoka *et al.*, 1995, Cochran *et al.*, 2004]. Ocean loading probably plays an important role in this case, with high tide likely serving to reduce the coupling force between the subducting and overriding plates by exerting a downward force on the subducting plate (the footwall) seaward of the trench [Cochran *et al.*, 2004]. The depth of the triggered events in this study (generally 30–35 km) means that the tidal stress is extremely small compared with the confining pressure. Therefore the fact that triggering occurs suggests the presence of near-lithostatic pore pressures in the tremor source region. Elevated pore pressures would serve to mitigate the effects of this depth by greatly reducing the effective normal stress on the fault, making the tidal stresses relatively more important. Tidal triggering of tremor has also been reported in eastern Shikoku [Nakata *et al.*, 2006], indicating that this behavior may be relatively common. A likely scenario is that tidal forces modulate the slip velocity in the region surrounding the LFE clusters, generating an increased LFE/tremor activity level during times when the slip rate in the surrounding region is accelerated.

### 3.4. Implications for the Mechanics of Tremor and Slip

[26] Although tremor appears to be generated by shear slip, fluids may play an important role in enabling such slip. This idea is supported by tomographic and seismic reflection studies suggesting high fluid pressures may be present in the tremor and slow slip zone [Shelly *et al.*, 2006; Kodaira *et al.*, 2004]. Kodaira *et al.* [2004] proposed that high fluid pressure could enable transient slip by extending the conditionally stable region between zones of velocity weakening updip and velocity strengthening downdip.

[27] Modeling studies also indicate that near-lithostatic fluid pressures may promote transient slip behavior [Liu and Rice, 2007], even without time-varying properties [Liu and Rice, 2005]. An alternate possibility is the existence of a transition in friction properties from velocity weakening behavior at very low slip speeds to velocity strengthening at higher velocities as modeled by Shibasaki and Iio [2003]. Observed triggering of tremor, both by seismic waves from distant earthquakes [Miyazawa and Mori, 2005; 2006; Rubinstein *et al.*, 2007] and by tidal stresses, further suggests that fluids play a role in this process, and that the system

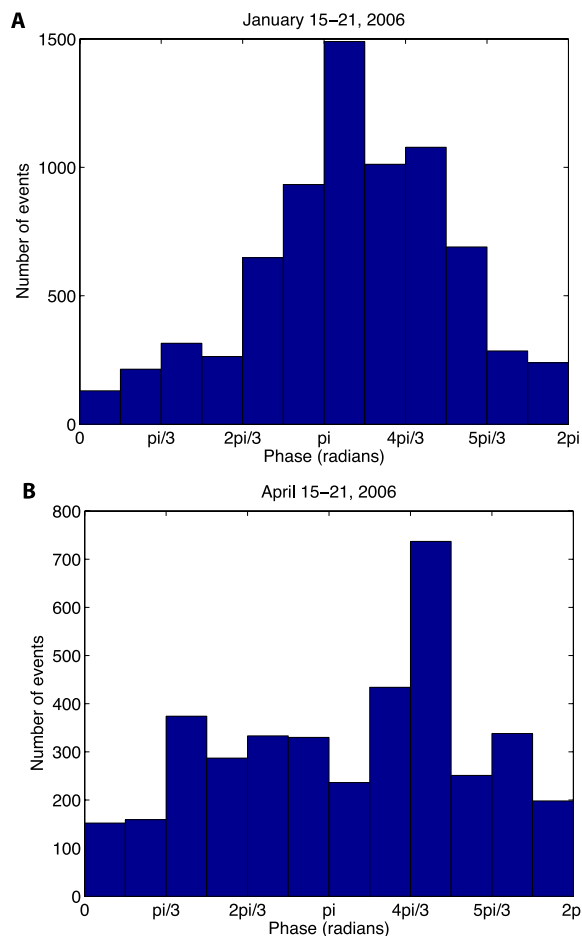


**Figure 19.** Histograms of LFE numbers versus phase angle, assuming a period of 12.4 hours (the average tidal period): (a) 15–21 January 2006 and (b) 15–21 April 2006. The phase angle is assigned to be zero at the beginning of each episode (i.e., at 0000 LT on 15 January and 15 April) and is repeated every 12.4 hours. The January event exhibits a very clear tidal triggering, while the tidal effect in the April event is less obvious.

may be sensitive to small perturbations in fluid pressure.

## 4. Conclusions

[28] Strong evidence supports the notion that non-volcanic tremor, at least in western Shikoku, is generated by shear slip on the plate interface. These micro-slips do not generally occur in isolation but rather in swarms as a cascade of shear failure along the plate boundary. The slip from these events clearly contributes the geodetically detected slip and thus slow slip and tremor can be considered essentially different manifestations of a single process. However, strong tremor activ-

ity is concentrated at certain areas of the plate boundary, where some heterogeneity in fluids, mineral properties, and/or geometry likely exists. As a result, these zones stick and slip as they are driven by slip in the surrounding region. Activity within one tremor cluster often propagates through the cluster, but takes a matter of minutes, rather than seconds as for a comparable earthquake rupture. Areas of the plate boundary between these strong tremor patches may slip while generating only weak (and possibly undetectable) tremor.

[29] Slow slip does not evolve smoothly, but rather contains of a series of subevents. These subevents are pulses of more rapid slip, such as the VLF events reported by *Ito et al.* [2007]. We also infer somewhat larger, slower subevents from precise tremor locations, propagating primarily in the along-dip direction at velocities of 20–150 km/hr. The relative scarcity of these subevents extending a significant distance along strike may be due to fault segmentation, perhaps reflecting a “grain” of the plate interface oriented in the dominant slip direction. In addition, tremor activity often demonstrates strong tidal periodicity, possibly reflecting the modulation of overall slip velocity of the transient event by tidal forces. This observation suggests that the high confining pressure expected at this depth is mitigated by near-lithostatic fluid pressure, resulting in very low effective normal stress on the plate interface.

## Acknowledgments

[30] We gratefully acknowledge Shutaro Sekine and Kazushige Obara of NIED for providing the graphics shown in Figure 2. Justin Rubinstein and Honn Kao provided helpful reviews. This material is based upon work supported by the National Science Foundation grant EAR-0409917. All data were obtained from the NIED Hi-net data server. This work utilized the Stanford Center for Computational Earth and Environmental Science.

## References

- Cochran, E. S., J. E. Vidale, and S. Tanaka (2004), Earth tides can trigger shallow thrust fault earthquakes, *Science*, *306*, 1164–1166.
- Dragert, H., K. Wang, and T. S. James (2001), A silent slip event on the deeper Cascadia subduction interface, *Science*, *292*, 1525–1528.
- Dragert, H., K. Wang, and G. Rogers (2004), Geodetic and seismic signatures of episodic tremor and slip in the northern Cascadia subduction zone, *Earth Planets Space*, *56*, 1143–1150.
- Gibbons, S. J., and F. Ringdal (2006), The detection of low magnitude seismic events using array-based waveform correlation, *Geophys. J. Int.*, *165*, 149–166.

- Hirose, H., K. Hirahara, F. Kimata, N. Fujii, and S. Miyazaki (1999), A slow thrust slip event following the two 1996 Hyuganada earthquakes beneath the Bungo Channel, southwest Japan, *Geophys. Res. Lett.*, *26*, 3237–3240.
- Ide, S., D. R. Shelly, and G. C. Beroza (2007a), Mechanism of deep low frequency earthquakes: Further evidence that deep non-volcanic tremor is generated by shear slip on the plate interface, *Geophys. Res. Lett.*, *34*, L03308, doi:10.1029/2006GL028890.
- Ide, S., G. C. Beroza, D. R. Shelly, and T. Uchide (2007b), A scaling law for slow earthquakes, *Nature*, *447*, 76–79, doi:10.1038/nature05780.
- Ito, Y., K. Obara, K. Shiomi, S. Sekine, and H. Hirose (2007), Slow earthquakes coincident with episodic tremors and slow slip events, *Science*, *315*, 503–506, doi:10.1126/science.1134454.
- Kao, H., S.-J. Shan, H. Dragert, G. Rogers, J. F. Cassidy, K. Wang, T. S. James, and K. Ramachandran (2006), Spatial-temporal patterns of seismic tremors in northern Cascadia, *J. Geophys. Res.*, *111*, B03309, doi:10.1029/2005JB003727.
- Kao, H., S.-J. Shan, G. Rogers, and H. Dragert (2007), Migration characteristics of seismic tremors in the northern Cascadia margin, *Geophys. Res. Lett.*, *34*, L03304, doi:10.1029/2006GL028430.
- Katsumata, A., and N. Kamaya (2003), Low-frequency continuous tremor around the Moho discontinuity away from volcanoes in the southwest Japan, *Geophys. Res. Lett.*, *30*(1), 1020, doi:10.1029/2002GL015981.
- Kodaira, S., T. Iidaka, A. Kato, J.-O. Park, T. Iwassaki, and Y. Kaneda (2004), High pore fluid pressure may cause silent slip in the Nankai Trough, *Science*, *304*, 1295–1298.
- Liu, Y., and J. R. Rice (2005), Aseismic slip transients emerge spontaneously in three-dimensional rate and state modeling of subduction earthquake sequences, *J. Geophys. Res.*, *110*, B08307, doi:10.1029/2004JB003424.
- Liu, Y., and J. R. Rice (2007), Spontaneous and triggered aseismic deformation transients in a subduction fault model, *J. Geophys. Res.*, *112*, B09404, doi:10.1029/2007JB004930.
- Miyazawa, M., and J. Mori (2005), Detection of triggered deep low-frequency events from the 2003 Tokachi-oki earthquake, *Geophys. Res. Lett.*, *32*, L10307, doi:10.1029/2005GL022539.
- Miyazawa, M., and J. Mori (2006), Evidence suggesting fluid flow beneath Japan due to periodic seismic triggering from the 2004 Sumatra-Andaman earthquake, *Geophys. Res. Lett.*, *33*, L05303, doi:10.1029/2005GL025087.
- Nadeau, R. M., and T. V. McEvilly (1999), Fault slip rates at depth from recurrence intervals of repeating microearthquakes, *Science*, *285*, 718–721, doi:10.1126/science.285.5428.718.
- Nakata, R., N. Suda, and H. Tsuruoka (2006), Tidal synchronicity of the low-frequency tremor in eastern Shikoku, Japan, *Eos Trans. AGU*, *87*(52), Fall Meet. Suppl., Abstract V41A-1700.
- Obara, K. (2002), Nonvolcanic deep tremor associated with subduction in southwest Japan, *Science*, *296*, 1679–1681.
- Obara, K., H. Hirose, F. Yamamizu, and K. Kasahara (2004), Episodic slow slip events accompanied by non-volcanic tremors in southwest Japan subduction zone, *Geophys. Res. Lett.*, *31*, L23602, doi:10.1029/2004GL020848.
- Ozawa, S., M. Murakami, M. Kaidzu, T. Tada, T. Sagiya, Y. Hatanaka, H. Yarai, and T. Nishimura (2002), Detection and monitoring of ongoing aseismic slip in the Tokai region, central Japan, *Science*, *298*, 1009–1012.
- Rogers, G., and H. Dragert (2003), Episodic tremor and slip on the Cascadia subduction zone: The chatter of silent slip, *Science*, *300*, 1942–1943.
- Rubin, A. M., D. Gillard, and J.-L. Got (1999), Streaks of microearthquakes along creeping faults, *Nature*, *400*, 635–641.
- Rubinstein, J. L., J. E. Vidale, J. Gomberg, P. Bodin, K. C. Kreager, and S. D. Malone (2007), Non-volcanic tremor driven by large transient shear stresses, *Nature*, *448*, 579–582, doi:10.1038/nature06017.
- Schaff, D. P., G. C. Beroza, and B. E. Shaw (1998), Postseismic response of repeating aftershocks, *Geophys. Res. Lett.*, *25*, 4549–4552.
- Schuster, A. (1897), On lunar and solar periodicities of earthquakes, *Proc. R. Soc. London*, *61*, 455–465.
- Sekine, S., and K. Obara (2006), A short-term slow slip event with deep low-frequency tremors at western part of Shikoku (April, 2006), *Rep. Coord. Comm. Earthquake Predict.*, *76*, 555–556.
- Seno, T., and T. Yamasaki (2003), Low-frequency tremors, intraslab and interplate earthquakes in Southwest Japan— from a viewpoint of slab dehydration, *Geophys. Res. Lett.*, *30*(22), 2171, doi:10.1029/2003GL018349.
- Shelly, D. R., G. C. Beroza, S. Ide, and S. Nakamura (2006), Low-frequency earthquakes in Shikoku, Japan and their relationship to episodic tremor and slip, *Nature*, *442*, 188–191, doi:10.1038/nature04931.
- Shelly, D. R., G. C. Beroza, and S. Ide (2007), Non-volcanic tremor and low frequency earthquake swarms, *Nature*, *446*, 305–307, doi:10.1038/nature05666.
- Shibazaki, B., and Y. Iio (2003), On the physical mechanism of silent slip events along the deeper part of the seismogenic zone, *Geophys. Res. Lett.*, *30*(9), 1489, doi:10.1029/2003GL017047.
- Tanaka, S., M. Ohtake, and H. Sato (2002), Evidence for tidal triggering of earthquakes as revealed from statistical analysis of global data, *J. Geophys. Res.*, *107*(B10), 2211, doi:10.1029/2001JB001577.
- Tsuruoka, H., M. Ohtake, and H. Sato (1995), Statistical test of the tidal triggering of earthquakes: Contribution of the ocean tide loading effect, *Geophys. J. Int.*, *122*, 183–194.
- Waldhauser, F., W. L. Ellsworth, D. P. Schaff, and A. Cole (2004), Streaks, multiplets, and holes: High-resolution spatio-temporal behavior of Parkfield seismicity, *Geophys. Res. Lett.*, *31*, L18608, doi:10.1029/2004GL020649.